

# SUB-GAUSSIAN ROTATION-INVARIANT FEATURES FOR STEERABLE WAVELET-BASED IMAGE RETRIEVAL

G. Tzagkarakis<sup>1</sup>, B. Beferull-Lozano<sup>2</sup>, and P. Tsakalides<sup>1</sup>

<sup>1</sup>Department of Computer Science, University of Crete and  
Institute of Computer Science - FORTH  
711 10 Heraklion, Crete, Greece  
gtzag@ics.forth.gr, tsakalid@ics.forth.gr

<sup>2</sup>School of Computer and Communication Sciences  
Swiss Federal Institute of Technology - EPFL  
CH1015, Lausanne, Switzerland  
Baltasar.Beferull@epfl.ch

## ABSTRACT

This paper presents a new rotation-invariant image retrieval method, which extends a recently introduced classification technique based on steerable wavelet transforms. In the proposed procedure, the feature extraction step consists of estimating the *covariations* (lower-order cross-correlations) between the wavelet subband coefficients, which are modeled as *sub-Gaussian* random vectors. The similarity measurement is carried out first by employing norms calculating the distance between the covariation matrices representing two distinct images and second by evaluating the Kullback-Leibler Distance (KLD) between their corresponding Sub-Gaussian distributions. We provide analytical expressions relating the sub-Gaussian features corresponding to a rotated image from the features of the original image. Finally, we relate the employed optimal lower-order correlation ( $p \leq 2$ ) to the degree of non-Gaussianity of the wavelet coefficients, and we demonstrate the effectiveness of our method using real texture images.

## 1. INTRODUCTION

During the last decades, digital images are being gathered and stored at an explosive rate on large digital information databases. This fact gives rise to the important issue of effectively and precisely searching and interacting with these collections. The purpose of an efficient content-based information retrieval system is to bring back all the relevant images from a specific database, given a user query. It goes without saying that retrieving images from unannotated database based on their visual content is a challenging problem.

In a typical Content-Based Image Retrieval (CBIR) system, we can distinguish two major tasks: Feature Extraction (FE) and Similarity Measurement (SM). In the FE

step, a set of features, constituting the so-called image signature, is generated to accurately represent the content of a given image. This set has to be much smaller in size than the original image while capturing as much as possible of the image information. During the SM step, a distance function is employed, which measures how close to a query image each image in the database is, in order to retrieve the "most relevant" images.

In the present work, texture information is used as a feature for representing the content of an image. Recently, Do and Vetterli applied a statistical framework in a wavelet-based texture retrieval application, by jointly considering the two problems of FE and SM [1]. In their approach, the FE step becomes an ML estimator for the model parameters of the wavelet coefficients in each subband, where they were independently modeled by a generalized Gaussian density (GGD). Then, the SM step computes the Kullback-Leibler distance between the model parameters.

In recent work, we have shown that successful modeling of the wavelet subband coefficients is achieved by taking into consideration the actual heavy-tailed behavior of their marginal densities [2]. Specifically, we have shown that the subband decompositions of many texture images have non-Gaussian statistics that are best described by families of distributions with algebraic tails, such as the Symmetric Alpha-Stable ( $S\alpha S$ ). After extracting the  $S\alpha S$  model parameters, we analytically derived and employed the KLD as the distance measure between two  $S\alpha S$  distributions. Our formulation improved the retrieving performance of the system, resulting in a decreased probability error rate for images with distinct non-Gaussian statistics.

However, both approaches in [1] and [2] do not take into account the possible interdependencies between different subbands (or equivalently orientations) of a given image, which can be employed in order to provide a more accurate representation of the texture image profile. Huang studied the correlation properties of wavelet transform coefficients at different subbands and resolution levels applying these properties on an image coding scheme based on neu-

---

This work was supported by the Greek General Secretariat for Research and Technology under Program EIIAN, Codes HIIA-011 and 1308/B1/3.3.1/317/12.04.2002.

ral networks [3]. Portilla and Simoncelli developed an algorithm for synthesizing texture images by setting different constraints on the correlation between the raw coefficients, their magnitudes, and other statistics [4].

Recently, a rotation-invariant image retrieval system based on steerable pyramids was proposed by Beferull-Lozano *et al.* [5]. In this system, the correlation matrices between the basic orientations at each level of the pyramid are chosen as the energy-based texture features. It is proven that the correlation matrix of a fixed level of the original image is equivalent to the corresponding correlation matrix of a rotated version of the same image. Taking this relation into account, the similarity measure between two images is defined as the minimum Frobenius norm, over all possible rotations  $\theta$ , of the difference between the correlation matrix of the original (query) image and that of each image in the database.

In the present work, we proceed by considering the wavelet subband coefficients at each decomposition level as samples of a sub-Gaussian random process. The sub-Gaussian model and the associated fractional lower-order statistics have been used in the past to develop data-adaptive algorithms for signal detection in impulsive interference [6, 7]. Within the framework of sub-Gaussian processes, we use the notion of covariation, instead of the second-order correlation, in order to extract possible interdependencies between wavelet coefficients at different image orientations. We derive analytical expressions for the relation between the covariation matrices of the original and the rotated images to directly obtain the features of the rotated image, given the features of the original image.

## 2. JOINT MODELING OF WAVELET SUBBAND COEFFICIENTS

In our data modeling study, we used textures (real-world  $512 \times 512$  natural scene images) obtained from the MIT Vision Texture (VisTex) and the Brodatz databases. We divided each image into  $16 \times 16 \times 16$  subimages and we employed three levels of decomposition. The statistical fitting of the marginal distribution of each subband proceeds in two steps: First, we assess whether the data deviate from the normal distribution and we determine if they have heavy tails by employing normal probability plots. Then, we check if the data is in the stable domain of attraction by estimating the characteristic exponent,  $\alpha$ , directly from the data and by providing the related confidence intervals. As further stability diagnostics, we employ the amplitude probability density (APD) curves ( $P(|X| > x)$ ) that give a good indication of whether the  $S\alpha S$  fit matches the data near the mode and on the tails of the distribution.

In this paper, we extract the interdependencies between pairs of subbands at each decomposition level by utilizing their joint statistics. For this purpose, we construct the vector with each component corresponding to a subband and we consider it as a sample of a so-called  $\alpha$ -sub-Gaussian process ( $\alpha$ -SG( $\mathbf{R}$ )), which is a variance mixture of a Gaussian process, defined as follows:

*Definition:* Let  $\{G(t), t \in T\}$  be a Gaussian process with covariance function  $R(u,v)$  and  $A \sim S_{\alpha/2}((\cos \frac{\pi\alpha}{4})^{2/\alpha}, 1, 0)$

be a positive  $\frac{\alpha}{2}$ -stable random variable where  $\alpha < 2$ . Assume that the random variable  $A$  is independent of  $\{G(t), t \in T\}$ . The  $S\alpha S$  process  $\{X(t) = A^{1/2}G(t), t \in T\}$  is a sub-Gaussian process with an underlying Gaussian process  $\{G(t), t \in T\}$ .

The finite dimensional projections,  $(X(t_1), \dots, X(t_d))$ ,  $d \geq 1$ , are  $\alpha$ -SG( $\mathbf{R}$ ) random vectors with underlying covariance matrix  $\mathbf{R}$ . For example, in the standard 2-D DWT with 3 subbands (H: horizontal, V: vertical, D: diagonal) we define these vectors as  $\vec{X} = [X_H, X_V, X_D]^T$ . Then, for the subbands at a specific level, we assume that the vectors  $\vec{X}_k = [X_{H,k}, X_{V,k}, X_{D,k}]^T$ ,  $k = 1, \dots, N$ , are samples taken from an  $\alpha$ -SG( $\mathbf{R}$ ) process where  $N$  is the number of pixels of each of the subbands and the subscript  $k$  goes through all the spatial locations of the subband.

The notion of covariance between two random variables plays an important role in the second-order moment theory. However, covariances do not exist for the family of  $S\alpha S$  random variables, due to the lack of finite variance. Instead, a quantity called *covariation*, which under certain constraints plays an analogous role for  $S\alpha S$  random variables to the one played by covariance for Gaussian random variables, has been proposed [8]. Let  $X$  and  $Y$  be jointly  $S\alpha S$  random variables with  $\alpha > 1$ , zero location parameters and dispersions  $\gamma_X$  and  $\gamma_Y$  respectively. The covariation of  $X$  with  $Y$  is defined by [8]

$$[X, Y]_\alpha = \frac{E\{XY^{<p-1>}\}}{E\{|Y|^p\}} \gamma_Y \quad (1)$$

where for any complex number  $z$  and  $a \geq 0$  we use the notation  $z^{<a>} = |z|^{a-1}\bar{z}$ , with  $\bar{z}$  denoting complex conjugation. We note that the covariation is defined in terms of the so-called *fractional lower order moments* (FLOM's) of a  $S\alpha S$  random variable  $Y$ ,

$$E\{|Y|^p\} = (c(p, \alpha) \cdot \gamma_Y)^p, \quad 0 < p < \alpha, \quad (2)$$

where

$$c(p, \alpha) = \frac{2^{p+1}\Gamma\left(\frac{p+1}{2}\right)\Gamma\left(-\frac{p}{\alpha}\right)}{\alpha\sqrt{\pi}\Gamma\left(-\frac{p}{2}\right)}.$$

## 3. FEATURE EXTRACTION

### 3.1. Case without rotations

In the FE stage of the proposed method we proceed in two steps: first we estimate the characteristic exponent of the sub-Gaussian process. This value can be estimated on the basis of the observation that each component in the sub-Gaussian vector is a  $S\alpha S$  random variable of the same characteristic exponent  $\alpha$  as the vector [8]. For instance, in the case described before we could estimate the  $\alpha$  parameter from the first components of each sub-Gaussian vector, i.e. from the set  $\{X_{H,k}\}_{k=1,\dots,N}$  containing the wavelet coefficients of the Horizontal subband (the previous observation indicates that under the sub-Gaussian assumption, the estimation could be realized using any of the sets  $\{X_{V,k}\}_{k=1,\dots,N}$ ,  $\{X_{D,k}\}_{k=1,\dots,N}$ ).

The second step of the proposed method consists of the estimation of the covariation matrix  $\mathbf{C}$ , with elements the covariations between the components of the  $\alpha$ -SG( $\mathbf{R}$ ) vectors, and the estimation of the underlying covariance matrix  $\mathbf{R}$ , corresponding to the Gaussian part of the  $\alpha$ -SG( $\mathbf{R}$ ) vectors. In the case of 3 subbands at each level, we consider the previously defined vectors  $\vec{X}_k = [X_{H,k}, X_{V,k}, X_{D,k}]^T$ ,  $k=1, \dots, N$  as independent realizations of an  $\alpha$ -SG( $\mathbf{R}$ ) process. Solving (2) with respect to  $\gamma_Y$ , substituting in (1) and replacing the expectation operators,  $E\{\cdot\}$ , with the sample means, we can estimate the elements  $C_{mn} = [X_m, X_n]_\alpha$  of the covariation matrix  $\mathbf{C}$  as follows (for convenience we set  $X_1 = X_H$ ,  $X_2 = X_V$ ,  $X_3 = X_D$ ):

$$\hat{C}_{mn} = (c(p, \alpha))^{-\frac{\alpha}{p}} \left[ \frac{1}{N} \sum_{k=1}^N X_m^k (X_n^k)^{\langle p-1 \rangle} \right] \left[ \frac{1}{N} \sum_{k=1}^N |X_n^k|^p \right]^{\frac{\alpha}{p}-1} \quad (3)$$

A second covariation estimator is obtained by replacing the expectation operators in (1) with the sample means and using an ML estimator for  $\gamma_Y$ :

$$\hat{C}_{mn}^{FLOM} = \frac{\sum_{k=1}^N X_m^k |X_n^k|^{p-1} \text{sign}(X_n^k)}{\sum_{k=1}^N |X_n^k|^p} \gamma_{X_n}^\alpha \quad (4)$$

The estimation of the covariations requires the specification of the arbitrary parameter  $p$ . We compute the optimal  $p$  as a function of the characteristic exponent  $\alpha$ , by computing the value of  $p$  that minimizes the standard deviation of the estimators for different values of  $\alpha > 1$ . For this purpose we studied the influence of the  $p$  parameter to the performance of the estimators given by (3), (4) via Monte-Carlo simulations. We generated two real  $S\alpha S$  ( $1 < \alpha \leq 2$ ) random variables,  $X$  and  $Y$ , as follows:

$$\begin{aligned} X &= a_1 U + b_1 V \\ Y &= a_2 U + b_2 V, \end{aligned}$$

where  $U$  and  $V$  are independent, standard ( $\gamma_U = \gamma_V = 1$ )  $S\alpha S$  random variables and  $\{a_i, b_i, i = 1, 2\}$  are real coefficients. We randomly selected these coefficients to be equal to

$$\begin{bmatrix} a_1 & b_1 \\ a_2 & b_2 \end{bmatrix} = \begin{bmatrix} 0.32 & -1.7 \\ -2.45 & 0.44 \end{bmatrix}.$$

We generated  $N = 5000$  independent samples of  $U$  and  $V$  and calculated the covariation estimator by means of (3), (4) for different values of  $p$  in the range  $(0, 2]$ . We ran  $K = 1000$  Monte-Carlo simulations for different values of  $\alpha \in (1, 2]$ , comparing the performance of the above two covariation estimators. Figure 1 displays the standard deviation of the estimator  $\hat{C}^{FLOM}(p)$  as a function of the parameter  $p$  and for different values of  $\alpha$ .

Table 1 shows comparative results on the performance of the two estimators. We include the mean of the estimators, the standard deviation in parentheses and the value of  $p$  for which the smallest standard deviation is achieved by the estimators. We observe that, in general, the two estimators have comparable performance, with the  $\hat{C}^{FLOM}(p)$  estimator resulting in a smaller standard deviation for most of the values of  $\alpha$ . This comparative performance of the covariation estimators is also similar when other values of the

$\alpha$	$\hat{C}(p)$	$\hat{C}^{FLOM}(p)$	True $[X, Y]_\alpha$
1.1	-1.9129 (0.1604)	-1.9158 (0.1397)	(p=0.56) -1.916
1.2	-1.8211 (0.1607)	-1.8203 (0.1390)	(p=0.57) -1.8254
1.3	-1.7476 (0.1476)	-1.755 (0.1481)	(p=0.59) -1.7476
1.4	-1.6913 (0.1472)	-1.6814 (0.1234)	(p=0.66) -1.6821
1.5	-1.6292 (0.1354)	-1.6201 (0.1218)	(p=0.68) -1.6285
1.7	-1.5614 (0.1156)	-1.5533 (0.1062)	(p=0.76) -1.5561
1.9	-1.5252 (0.0954)	-1.5109 (0.0886)	(p=0.91) -1.5288
2	-1.5324 (0.0640)	-1.5301 (0.0668)	(p=2) -1.532

**Table 1.** Performance of the covariation estimators.

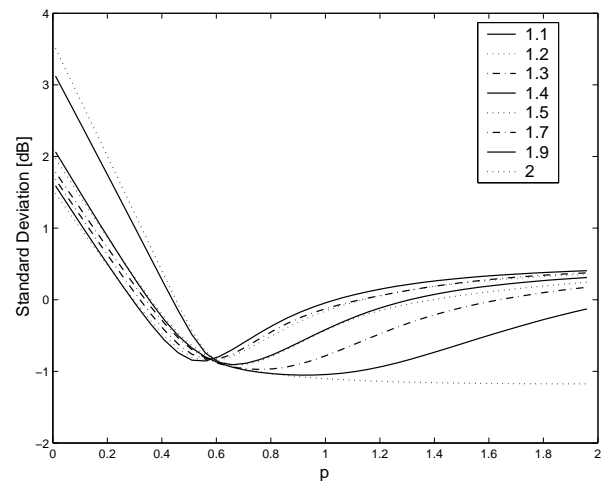


**Fig. 1.** Curves representing the standard deviation of the covariation estimation as a function of the parameter  $p$  for the  $\hat{C}^{FLOM}$  estimator.

coefficients  $\{a_i, b_i, i = 1, 2\}$  are used. Thus, in our experimental evaluations we will rely on this estimator.

For a given  $\alpha_k$ , we repeated the simulations for different pairs of  $(\gamma_U, \gamma_V)$  and we defined the optimal  $p$  value associated with  $\alpha_k$  as the mean of the optimal  $p$  values corresponding to each  $(\gamma_U, \gamma_V)$  pair.

Then, we can estimate the elements  $R_{mn}$  of the underlying covariance matrix using the relation

$$C_{mn} = 2^{-\frac{\alpha}{2}} R_{mn} R_{nn}^{\frac{\alpha-2}{2}} \quad (5)$$

resulting in the following estimators

$$\hat{R}_{nn} = [2^{\frac{\alpha}{2}} \hat{C}_{nn}]^{\frac{2}{\alpha}}, \quad \hat{R}_{mn} = 2^{\frac{\alpha}{2}} \frac{\hat{C}_{mn}}{\hat{R}_{nn}^{\frac{\alpha-2}{2}}}, \quad (6)$$

which are consistent and asymptotically normal.

### 3.2. Case with rotations

In the case of a database containing images along with rotated versions of them, we are interested in finding features which are as "steerable" as possible, that is given the features of an image oriented at an angle  $\phi$ , we should be able to obtain the features corresponding to the same image rotated at an angle  $\theta$ , without having to re-extract the features after the rotation.

Let  $c(x_k, \phi)$  represent the value of a transform coefficient at a spatial location  $x_k$  and orientation  $\phi$ . In a steerable pyramid with  $J$  basic orientations (subbands) and  $L$  levels, at each level  $l$ , given the  $J$  basic coefficients

$$\{c^l(x_k, \phi_1), c^l(x_k, \phi_2), \dots, c^l(x_k, \phi_J)\}$$

the transform coefficient  $c^l(x_k, \phi)$  for any angle  $\phi$  is given by [5]:

$$c^l(x_k, \phi) = \sum_{i=1}^J f_i(\phi) c^l(x_k, \phi_i) \quad \forall \phi, \quad l = 1, \dots, L \quad (7)$$

where  $\{f_1(\phi), f_2(\phi), \dots, f_J(\phi)\}$  is the set of  $J$  steering functions.

Under the sub-Gaussian assumption, the  $J$  basic coefficients at a level  $l$  can be expressed as:

$$c^l(x_k, \phi_i) = A^{1/2} c_G^l(x_k, \phi_i), \quad i = 1, \dots, J \quad (8)$$

where  $c_G^l(x_k, \phi_i)$  is the Gaussian part of the  $\alpha$ -SG( $\mathbf{R}$ ) vector. From (7) the transform coefficient at any angle  $\phi$  is given by:

$$c^l(x_k, \phi) = A^{1/2} \sum_{i=1}^J f_i(\phi) c_G^l(x_k, \phi_i) \quad (9)$$

$$= A^{1/2} c_G^l(x_k, \phi) \quad (10)$$

(10) shows that the transform coefficients of a rotated image at an angle  $\phi$  are also sub-Gaussian random variables with the same characteristic exponent with that of the original image, and a Gaussian part which corresponds to the same angle  $\phi$ . Let  $\mathbf{R}$ ,  $\mathbf{R}_\theta$  denote the underlying covariance matrices of the original image and its rotation at an angle  $\theta$ , respectively. Proposition 1 in [5] indicates that  $\mathbf{R}$  and  $\mathbf{R}_\theta$  are equivalent matrices, i.e., they can be written in the form:

$$\mathbf{R}_\theta = \mathbf{A}(\theta) \mathbf{R} \mathbf{A}^T(\theta) \quad (11)$$

where

$$\mathbf{A}(\theta) = \begin{bmatrix} f_1(\phi_1 - \theta) & f_2(\phi_1 - \theta) & \dots & f_J(\phi_1 - \theta) \\ f_1(\phi_2 - \theta) & f_2(\phi_2 - \theta) & \dots & f_J(\phi_2 - \theta) \\ \vdots & \vdots & \ddots & \vdots \\ f_1(\phi_J - \theta) & f_2(\phi_J - \theta) & \dots & f_J(\phi_J - \theta) \end{bmatrix}$$

(5) gives the relation between the elements of the covariation matrix  $\mathbf{C}_\theta$  of the rotated image and the corresponding elements of the underlying covariation matrix  $\mathbf{R}_\theta$ :

$$[\mathbf{C}_\theta]_{mn} = 2^{-\frac{\alpha}{2}} [\mathbf{R}_\theta]_{mn} ([\mathbf{R}_\theta]_{nn})^{\frac{\alpha-2}{2}} \quad (12)$$

By employing (11), (12) and after some manipulation the relation between the estimated covariation matrix  $\hat{\mathbf{C}}$  of the

original image and the corresponding estimated matrix  $\hat{\mathbf{C}}_\theta$  of its rotated version is given by:

$$\hat{\mathbf{C}}_\theta = \mathbf{M} \cdot * D(\mathbf{M}), \quad (13)$$

where

$$\mathbf{M} = \mathbf{A}(\theta) \hat{\mathbf{C}}' \mathbf{A}^T(\theta),$$

$$\hat{\mathbf{C}}' = \begin{bmatrix} \frac{\hat{\mathbf{C}}_{11}}{\hat{\mathbf{C}}_{11}^{(\alpha-2)/\alpha}} & \frac{\hat{\mathbf{C}}_{12}}{\hat{\mathbf{C}}_{22}^{(\alpha-2)/\alpha}} & \dots & \frac{\hat{\mathbf{C}}_{1J}}{\hat{\mathbf{C}}_{JJ}^{(\alpha-2)/\alpha}} \\ \vdots & \vdots & \ddots & \vdots \\ \frac{\hat{\mathbf{C}}_{J1}}{\hat{\mathbf{C}}_{11}^{(\alpha-2)/\alpha}} & \frac{\hat{\mathbf{C}}_{J2}}{\hat{\mathbf{C}}_{22}^{(\alpha-2)/\alpha}} & \dots & \frac{\hat{\mathbf{C}}_{JJ}}{\hat{\mathbf{C}}_{JJ}^{(\alpha-2)/\alpha}} \end{bmatrix},$$

$$D(\mathbf{M}) = \begin{bmatrix} \{\text{diag}(\mathbf{M})\} \cdot \wedge \left(\frac{\alpha-2}{2}\right) \\ \vdots \\ \{\text{diag}(\mathbf{M})\} \cdot \wedge \left(\frac{\alpha-2}{2}\right) \end{bmatrix}, \quad (14)$$

with  $(\cdot, *)$ ,  $(\cdot, \wedge)$  denoting element-by-element multiplication and element-by-element involution, respectively, and  $\text{diag}(M)$  is a row vector containing the main diagonal of the square matrix  $M$ . Notice also that the dimension of all the above matrices is equal to  $J \times J$ .

## 4. SIMILARITY MEASUREMENT

### 4.1. Case without rotations

In the FE step, we represent the texture information of an image using the covariation matrix for each decomposition level. A way to measure the distance between two corresponding levels of two distinct images, is to take a matrix norm of the difference of the two covariation matrices. In the similarity measurement step, the overall distance between two images  $I_1, I_2$  is given as the sum of the distances between the corresponding decomposition levels:

$$D(I_1, I_2) = \sum_{l=1}^L \|\mathbf{C}_{I_1}^l - \mathbf{C}_{I_2}^l\| \quad (15)$$

where  $L$  is the number of decomposition levels and  $\|\cdot\|$  may be anyone of the commonly used matrix norms.

Another way to measure the similarity between two images, is to proceed as in [2] by computing the KLD between the normalized multivariate characteristic functions corresponding to the  $\alpha$ -SG( $\mathbf{R}$ ) process at each decomposition level. This is an issue that we are currently studying.

### 4.2. Case with rotations

In the case that we permit a database containing rotated versions of the original images, one way to measure the similarity between the images is to proceed as in [5]. Then, the distance between two images  $I_1, I_2$  is defined as:

$$D(I_1, I_2) = \min_{\theta} \sum_{l=1}^L \|\mathbf{C}_{I_1}^l - \tilde{\mathbf{C}}_{I_2}^l\| \quad (16)$$

where

$$\tilde{\mathbf{C}}_{I_2}^l = 2^{-\alpha/2} \cdot (\tilde{\mathbf{R}}_{I_2}^l \cdot * D(\tilde{\mathbf{R}}_{I_2}^l)),$$

with

$$\tilde{\mathbf{R}}_{I_2}^l = \mathbf{A}(-\theta) \mathbf{R}_{I_2}^l \mathbf{A}^T(-\theta),$$

and

$$\mathbf{R}_{I_2}^l = 2 \cdot (\mathbf{C}_{I_2}^l .* \bar{D}(\mathbf{C}_{I_2}^l)) .$$

The operator  $\bar{D}(\mathbf{M})$  is equal to  $D(\mathbf{M}) \wedge (-2/\alpha)$ , where  $D(\cdot)$  is defined in (14). As before, all the above matrices are of dimension  $J \times J$ . The rotation-invariant Frobenius distance defined in (16) is derived by solving (13) with respect to  $\hat{\mathbf{C}}$ . As we may have a database of images along with rotated versions of them, we assume that  $I_2$  is a counter-clockwise rotation of the given query  $I_1$ . So, the signature of image  $I_2$  contains the estimated covariation matrices of the steerable model corresponding to  $I_2$ , given by (13).

The meaning of this similarity function is that before measuring the similarity between  $I_1$  and  $I_2$  we have to align them, that is, to rotate clockwise the signature of  $I_2$ . This clockwise rotation is expressed by the term  $\hat{\mathbf{C}}_{I_2}^l$ . Since we do not know the angle which gives the best alignment, we have to search over a set of possible rotations and this is expressed by the minimization operation over  $\theta$ . When  $I_1$ ,  $I_2$  are two rotated versions of the same image, the angle  $\theta_o$  for which the minimum is achieved in (16) must be close to the relative angle between  $I_1$  and  $I_2$ .

## 5. EXPERIMENTAL RESULTS

In order to evaluate the efficiency, the proposed retrieval scheme was applied on a set of 10,  $512 \times 512$  texture images. Each of them was physically rotated at 30, 60, 90 and 120 degrees, resulting in a set of 65 texture samples. Then, we divided each image into 4,  $256 \times 256$  non-overlapping subimages constructing a database with a total of  $4 \times 50 = 200$  textures. We implemented a 3-level steerable pyramid decomposition, by employing the following oriented basis (steering) functions:

$$f_1(\theta) = \frac{1}{2}[\cos(\theta) + \cos(3\theta)] \quad f_2(\theta) = f_1\left(\frac{\pi}{4} - \theta\right)$$

$$f_3(\theta) = f_1\left(\frac{\pi}{2} - \theta\right) \quad f_4(\theta) = f_1\left(\frac{3\pi}{4} - \theta\right)$$

with basic angles  $\phi_1 = 0$ ,  $\phi_2 = \pi/4$ ,  $\phi_3 = \pi/2$ ,  $\phi_4 = 3\pi/4$ , resulting in 4 oriented subbands at each level.

In this setup, the query is anyone of the subimages corresponding to the original, non-rotated images. The relevant images for each query are defined as the other 16 subimages corresponding to the rotated versions of the same original image. Figure 2 shows the average percentages of retrieving relevant subimages as a function of the number of top matches using the proposed steerable model, compared with the model that uses the covariance matrices as the extracted features together with the corresponding rotation-invariant version of the Frobenius norm [5]. The average retrieval rate of the proposed method is equal to 93%, while the corresponding rate for the method that makes a Gaussian assumption is equal to 83.75%.

As a conclusion, the proposed rotation-invariant retrieval scheme that takes into account the true heavy-tailed behavior of the marginal distribution of the pyramid subband coefficients and employs a joint sub-Gaussian model exploiting the high dependence across subbands, results in an

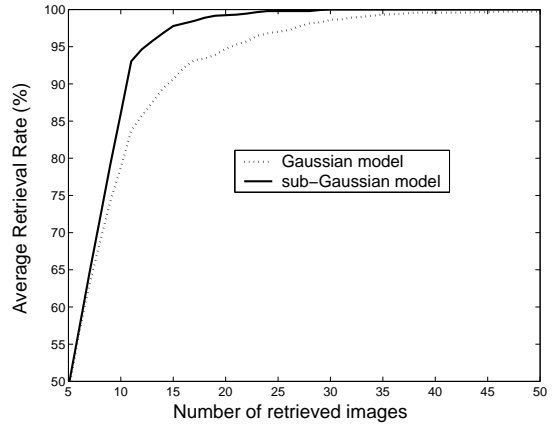


**Fig. 2.** Retrieval performance according to the number of top matches considered.

increased performance and a faster convergence rate compared with the rotation-invariant model that makes a Gaussian assumption for the joint distribution by computing  $2^{nd}$  order correlations.

## 6. REFERENCES

- [1] M. N. Do and M. Vetterli, "Wavelet-based texture retrieval using generalized Gaussian density and Kullback-Leibler distance," *IEEE Trans. Image Processing*, vol. 11, pp. 146–158, Feb. 2002.
- [2] G. Tzagkarakis and P. Tsakalides, "A statistical approach to texture image retrieval via alpha-stable modeling of wavelet decompositions," *5th International Workshop on Image Analysis for Multimedia Interactive Services, Lisboa, Portugal*, April 21-23 2004.
- [3] J. Huang, "Study on the correlation properties of wavelet transform coefficients and the applications in a neural network-based hybrid image coding system," *CISST'03, Las Vegas, USA*, June 22-26 2003.
- [4] J. Portilla and E. P. Simoncelli, "A parametric texture model based on joint statistics of complex wavelet coefficients," *International Journal of Computer Vision*, vol. 40, pp. 49–71, Dec. 2000.
- [5] B. Beferull-Lozano, H. Xie, and A. Ortega, "Rotation-invariant features based on steerable transforms with an application to distributed image classification,"
- [6] G. A. Tsihrintzis and C. L. Nikias, "Data adaptive algorithms for signal detection in sub-gaussian impulsive interference," *IEEE Trans. Signal Processing*. submitted on January, 1996, pp. 25.
- [7] G. A. Tsihrintzis and C. L. Nikias, "Robust signal detection and classification based on fractional lower-order statistics," *IEEE Trans. Signal Processing*. submitted on April, 1995, pp. 36.
- [8] G. Samorodnitsky and M. S. Taqqu, *Stable Non-Gaussian Random Processes: Stochastic Models with Infinite Variance*. New York: Chapman and Hall, 1994.